A Joint Radar-Communication Precoding Design Based on Cramér-Rao Bound Optimization

Fan Liu*, Ya-Feng Liu†, Christos Masouros‡, Ang Li§, and Yonina C. Eldar¶
*Southern University of Science and Technology, Shenzhen, China
†Academy of Mathematics and Systems Science, Chinese Academy of Sciences, Beijing, China
‡University College London, London, UK
§Xi'an Jiaotong University, Xi'an, China
¶Weizmann Institute of Science, Rehovot, Israel
Email: liuf6@sustech.edu.cn

***Abstract*—This paper investigates joint radar-communication (JRC) transmission, where a JRC precoder is designed to simultaneously perform target sensing and information signaling. We minimize the Cramér-Rao Bound (CRB) for target estimation, while guaranteeing the per-user signal-to-interference-plus-noise ratio (SINR) in the downlink. While the formulated problem is non-convex in general, we propose an efficient successive convex approximation (SCA) method, which solves a second-order cone program (SOCP) subproblem at each iteration. Numerical results demonstrate the effectiveness of the proposed JRC precoding design, showing that the SCA algorithm is able to approach the convex relaxation bound, which significantly outperforms conventional benchmark solvers in terms of both complexity and performance.**

***Index Terms*—Joint radar-communication, Cramér-Rao bound, semidefinite relaxation, successive convex approximation.**

I. Introduction

Joint radar-communications (JRC) transmission has recently been envisioned as a key enabling technology for a variety of emerging applications, such as intelligent transportation, indoor localization and sensing, and unmanned aerial vehicular (UAV) networks. Indeed, integrating radar sensing functionality into the next-generation wireless infrastructure, including not only beyond-5G and 6G, but also WiFi-7 networks, has been regarded as an important air interface technique [1]. On one hand, combining radar and communications leads to significant improvement in the spectral-, energy-, and hardware-efficiency, as the wireless resources and devices are resued to serve dual purposes. In addition, the two functionalities are able to assist each other in various ways, i.e., radar-assisted communications, and communication-assisted sensing, thus to achieve mutual benefits [2].

Waveform design plays an essential role in JRC systems, which aims at designing an unified waveform that is capable of both target sensing and information delievering. In general, there are three design methodologies for JRC waveforms, radar-centric design, communication-centric design, and joint design. Radar-centric design implements communication functionality into radar infrastructures by modifying dedicated radar signals. Representative radar-centric techniques include sidelobe control for MIMO radar, i.e., to embed communication bits in the sidelobes, while exploiting the mainlobe for target sensing solely [3]. On top of that, it is also viable to represent communication data by frequency and antenna index modulation, via using either a carrier agile phased-array radar (CAESAR) or a frequency-modulated continuous wave radar, leading to the multi-carrier agile joint radar-communication (MAJoRCom) or the FMCW radar-communication (FRaC) approach [4]–[6]. Communication-centric waveform designs, on the other hand, are mostly built upon standard-compatible communication waveforms and frame structures, e.g., using orthogoal frequency division multiplexing (OFDM) communication waveform for target detection [7], or exploiting the channel estimation field (CEF) in the IEEE 802.11ad frame, a WLAN protocol, for vehicle sensing [8], [9].

While both radar- and communication-centric designs realize JRC to a certain extent, they generally fail to formulate a scalable performance tradeoff between the dual functionalities. For instance, the radar-centric design typically employs interpulse modulation, resulting in a transmission data rate at the order of the pulse repetition frequency (PRF), which supports only limited communication applications. Moreover, due to the fact that the communication waveform and its frame structure are not tailored for radar, the radar sensing performance in communication-centric design may not be optimal. To overcome the above challenges, it would be more favorable to consider joint design approaches, which do not rely on existing radar or communication waveforms, but are conceived from the ground-up.

Among many joint design approaches, a classical method is waveform approximation, which simultaenously optimizes communication performance metrics, and imposes a waveform similarity constraint or objective function between the JRC waveform and a benchmark radar waveform, e.g., a chirp signal [10], [11]. By doing so, the JRC waveform may approach the benchmark radar performance. It is worth pointing out that, however, such methods may not be able to reach the JRC optimal performance bound, as the radar performance is implicitly guaranteed, rather than being directly optimized. As a further step, a joint precoding design has been proposed in [12] for multi-user multi-input multi-output (MU-MIMO) JRC system, which minimizes the CRB of target sensing, an

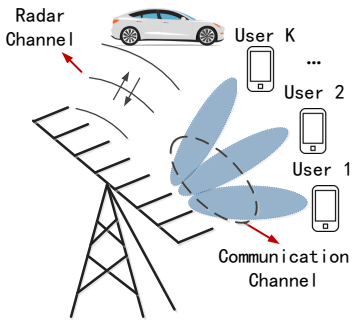

Fig. 1. Joint Radar-Communication Downlink System.

estimation metric, subject to per-user SINR constraints. In particular, the precoding design in [12] is formulated into a non-convex optimization problem, which is then relaxed into a convex problem by leveraging the semidefinite relaxation (SDR) method [13].

In this paper, we develop a successive convex approximation (SCA) algorithm to efficiently solve the non-convex JRC precoding problem in [12], which bypassing the need of formulating the SDR problem as well as the associated high computational overheads. In each iteration, the SCA algorithm solves an SOCP subproblem, which is known to have much lower complexity than that of solving the semidefinite program (SDP) with the same size. Numerical results show that the proposed SCA framework generates near-optimal solutions by approaching the SDR bound.

The remainder of this paper is organized as follows. Section II introduces the JRC system model. Section III formulates the precoding problem and develops an SCA solver. Section IV provides numerical results to verify the performance of the algorithm. Finally, Section V concludes the paper.

II. System Model

We consider a MIMO JRC base station (BS) equipped with N_t transmit antennas and N_r receive antennas, which is serving K downlink single-antenna users while detecting targets as a monostatic radar, as depicted in Fig. 1. Without loss of generality, we assume $K < N_t$. Before formulating the JRC precoding problem, we elaborate on the system model and performance metrics of both radar and communications.

A. Signal Model

Let $\mathbf{X} \in \mathbb{C}^{N_t \times L}$ be a JRC signal matrix, with $L > N_t$ being the length of the radar pulse/communication frame. By transmitting $\mathbf{X}$, the reflected echo signal matrix at the JRC BS is given by

$$\mathbf{Y}_R = \mathbf{G}\mathbf{X} + \mathbf{Z}_R, \tag{1}$$

where $\mathbf{Z}_R \in \mathbb{C}^{N_r \times L}$ denotes an additive white Gaussian noise (AWGN) matrix, with the variance of each entry being σ_R^2, and $\mathbf{G} \in \mathbb{C}^{N_r \times N_t}$ represents the target response matrix (TRM) [14].

The matrix $\mathbf{G}$ can be of different forms depending on the sensing scenarios, and adopted target models. For example, given an angular-spread extended target within a single range-Doppler bin, $\mathbf{G}$ can be expressed as

$$\mathbf{G} = \sum_{i=1}^{N_s} \alpha_i \mathbf{b}\left(\theta_i\right) \mathbf{a}^H\left(\theta_i\right), \tag{2}$$

where N_s is the number of resolvable scatterers on the extended target, α_i and θ_i denote the reflection coefficient and the angle of the i-th scatterer, and $\mathbf{a}\left(\theta\right)$ and $\mathbf{b}\left(\theta\right)$ are transmit and receive steering vectors, respectively.

Another example is to detect multiple point targets using OFDM waveforms. Suppose that the radar receives echoes from N_s point targets. Each target has individual reflection coefficient, angle, delay, and Doppler parameters $\alpha_i, \theta_i, \tau_i$, and $f_{D,i}$. Then $\mathbf{G}$ can be modeled as a TRM defined on the n-th subcarrier and the m-th OFDM symbol as

$$\mathbf{G} \triangleq \mathbf{G}_{n,m} = \mathbf{B}\left(\Theta\right) \mathbf{C}_n \mathbf{D}_m \mathbf{A}^H\left(\Theta\right), \tag{3}$$

where

$$\mathbf{A}\left(\Theta\right) = \left[\mathbf{a}\left(\theta_1\right), ..., \mathbf{a}\left(\theta_{N_s}\right)\right], \mathbf{B}\left(\Theta\right) = \left[\ \mathbf{b}\left(\theta_1\right), ..., \mathbf{b}\left(\theta_{N_s}\right)\right] \tag{4}$$

are transmit and receive steering matrices, and

$$\begin{aligned} \mathbf{C}_n &= \operatorname{diag}\left\{\left[\alpha_1 e^{-j2\pi(n-1)\Delta f \tau_1}, ..., \alpha_L e^{-j2\pi(n-1)\Delta f \tau_{N_s}}\right]\right\}, \\ \mathbf{D}_m &= \operatorname{diag}\left\{\left[e^{j2\pi f_{D,1}(m-1)T_{\mathrm{OFDM}}}, ..., e^{j2\pi f_{D,N_s}(m-1)T_{\mathrm{OFDM}}}\right]\right\} \end{aligned} \tag{5}$$

are phase shifting matrices caused by time delay and Doppler of each target, with Δf and T_{OFDM} represent subcarrier spacing and OFDM symbol duration.

To ensure the generality of the proposed method, in this paper, we consider a generic TRM $\mathbf{G}$, rather than restricting to a specific target model mentioned above. That is to say, we regard $\mathbf{G}$ as an unstructured TRM that contains useful information about the target, which is directly estimated from the echo signal $\mathbf{Y}$ as an unknown variable. The investigation of specific target models, e.g., (2) and (3), is designated as our future work.

The same JRC waveform $\mathbf{X}$ is also transmitted to K communication users. The received signal matrix at communication users is given as

$$\mathbf{Y}_C = \mathbf{H}\mathbf{X} + \mathbf{Z}_C, \tag{6}$$

where $\mathbf{Z}_C \in \mathbb{C}^{K \times L}$ is AWGN with the variance of each entry being σ_C^2, and $\mathbf{H} = \left[\mathbf{h}_1, \mathbf{h}_2, \ldots, \mathbf{h}_K\right]^H \in \mathbb{C}^{K \times N_t}$ represents the communication channel matrix, which is assumed to be perfectly estimated and is known to the BS. Moreover, $\mathbf{X}$ can be further given by

$$\mathbf{X} = \mathbf{W}_D \mathbf{S}_C, \tag{7}$$

where $\mathbf{W}_D$ is the dual-functional precoding matrix to be designed, and $\mathbf{S}_C \in \mathbb{C}^{K \times L}$ contains K unit-power data streams intended for the K users. The data streams are assumed to be orthogonal to each other so that

$$\frac{1}{L} \mathbf{S}_C \mathbf{S}_C^H = \mathbf{I}_K. \tag{8}$$

We define

$$\mathbf{R}_X = \frac{1}{L}\mathbf{X}\mathbf{X}^H = \frac{1}{L}\mathbf{W}_D\mathbf{S}_C\mathbf{S}_C^H\mathbf{W}_D^H = \mathbf{W}_D\mathbf{W}_D^H \quad (9)$$

as the sample covariance matrix of $\mathbf{X}$.

B. CRB for Radar Sensing

It is well-known that the CRB serves as a lower-bound of the variance of unbiased estimators for parameter estimation [15]. In this paper, we minimize the CRB so that the target estimation error can be reduced.

Let $\mathbf{y}_R = \mathrm{vec}\,(\mathbf{Y}_R)$, $\mathbf{g} = \mathrm{vec}\,(\mathbf{G})$, $\mathbf{z}_R = \mathrm{vec}\,(\mathbf{Z}_R)$, and define $\mathbf{v} = \left[\mathbf{g}_R^T, \mathbf{g}_I^T\right]^T$, where $\mathbf{g}_R$ and $\mathbf{g}_I$ are the real and imaginary parts of $\mathrm{vec}\,(\mathbf{G})$. One can rewrite (1) as

$$\mathbf{y}_R = \mathrm{vec}\,(\mathbf{G}\mathbf{X}) + \mathrm{vec}\,(\mathbf{Z}_R) = \left(\mathbf{X}^T \otimes \mathbf{I}_{N_r}\right)\mathbf{g} + \mathbf{z}_R. \quad (10)$$

Due to Gaussian distributed noise $\mathbf{z}_R$, the Fisher Information Martrix (FIM) with respect to $\mathbf{v}$ can be calculated as

$$[\mathbf{J}]_{ij} = \frac{2}{\sigma_R^2}\,\mathrm{Re}\left(\mathrm{tr}\left(\frac{\partial\left(\left(\mathbf{X}^T \otimes \mathbf{I}_{N_r}\right)\mathbf{g}\right)^H}{\partial v_i}\frac{\partial\left(\mathbf{X}^T \otimes \mathbf{I}_{N_r}\right)\mathbf{g}}{\partial v_j}\right)\right), \quad (11)$$

where $[\mathbf{J}]_{ij}$ is the (i,j)-th entry of $\mathbf{J}$, and v_i is the i-th entry of $\mathbf{v}$. Then we have

$$\begin{aligned}\mathbf{J} &= \frac{2}{\sigma_R^2}\begin{bmatrix}\mathrm{Re}\left(\mathbf{X}^*\mathbf{X}^T \otimes \mathbf{I}_{N_r}\right) & -\mathrm{Im}\left(\mathbf{X}^*\mathbf{X}^T \otimes \mathbf{I}_{N_r}\right)\\ \mathrm{Im}\left(\mathbf{X}^*\mathbf{X}^T \otimes \mathbf{I}_{N_r}\right) & \mathrm{Re}\left(\mathbf{X}^*\mathbf{X}^T \otimes \mathbf{I}_{N_r}\right)\end{bmatrix}\\ &= \frac{2L}{\sigma_R^2}\begin{bmatrix}\mathrm{Re}\left(\mathbf{R}_X^T \otimes \mathbf{I}_{N_r}\right) & -\mathrm{Im}\left(\mathbf{R}_X^T \otimes \mathbf{I}_{N_r}\right)\\ \mathrm{Im}\left(\mathbf{R}_X^T \otimes \mathbf{I}_{N_r}\right) & \mathrm{Re}\left(\mathbf{R}_X^T \otimes \mathbf{I}_{N_r}\right)\end{bmatrix},\end{aligned} \quad (12)$$

which is the real representation of $\frac{2L}{\sigma_R^2}\mathbf{R}_X^T \otimes \mathbf{I}_{N_r}$. Then, the CRB for each parameter can be obtained as the diagonal entries of the inverse of $\mathbf{J}$.

By examining (7) we see that $\mathbf{X} \in \mathbb{C}^{N_t \times L}$ is rank-deficient, since

$$\mathrm{rank}\,(\mathbf{X}) \le \min\left\{\mathrm{rank}\,(\mathbf{W}_D), \mathrm{rank}\,(\mathbf{S}_C)\right\} = K < N_t \le L. \quad (13)$$

Consequently, if we transmit only K signal streams, the Degrees-of-Freedom (DoFs) available are not enough to recover the rank-N_t matrix $\mathbf{G}$. Moreover, the FIM $\mathbf{J}$ becomes singular, resulting in the non-existence of the unbiased estimator according to [16], [17]. While one may constrain $\mathbf{G}$ into some subset, and employ a modified CRB [17], this leads to inevitable performance loss for target estimation, due to the lack of radar DoFs.

In order to guarantee satisfactory radar performance, we propose introducing an extra structure to $\mathbf{X}$ for extending the DoFs to its maximum, i.e., N_t, by transmitting dedicated probing streams in addition to data streams intended for K users. Note that these signal streams are dedicated to target probing, without carrying the communication data. Let us consider an augmented data matrix, given as

$$\tilde{\mathbf{S}} = \begin{bmatrix}\mathbf{S}_C\\ \mathbf{S}_A\end{bmatrix} \in \mathbb{C}^{N_t \times L}, \quad (14)$$

where $\mathbf{S}_A \in \mathbb{C}^{(N_t-K)\times L}$ denotes the dedicated probing streams, and is orthogonal to $\mathbf{S}_C$. Therefore, for sufficiently large L, it still holds true that

$$\frac{1}{L}\tilde{\mathbf{S}}\tilde{\mathbf{S}}^H = \mathbf{I}_{N_t}. \quad (15)$$

We further augment the precoding matrix in the form of

$$\tilde{\mathbf{W}}_D = [\mathbf{w}_1, \mathbf{w}_2, \ldots, \mathbf{w}_{N_t}] = [\mathbf{W}_C, \mathbf{W}_A] \in \mathbb{C}^{N_t \times N_t}, \quad (16)$$

where $\mathbf{W}_C = [\mathbf{w}_1, \ldots, \mathbf{w}_K] \in \mathbb{C}^{N_t \times K}$ is the communication precoder, and $\mathbf{W}_A = [\mathbf{w}_{K+1}, \ldots, \mathbf{w}_{N_t}] \in \mathbb{C}^{N_t \times (N_t-K)}$ is the auxiliary precoding matrix for the probing streams. By properly designing $\tilde{\mathbf{W}}_D$, the resulting transmitted signal matrix $\mathbf{X} = \tilde{\mathbf{W}}_D\tilde{\mathbf{S}}$ will have a full rank of N_t. Note that in this JRC signal model, the overall precoder $\tilde{\mathbf{W}}_D$ is used for sensing the target, for guaranteeing the estimation performance and the feasibility of unbiased estimation. The first K columns of $\tilde{\mathbf{W}}_D$, i.e., $\mathbf{W}_C$, convey information data to K users.

Based on the above, the sample covariance matrix of $\mathbf{X}$ is given by

$$\mathbf{R}_X = \tilde{\mathbf{W}}_D\tilde{\mathbf{W}}_D^H = \mathbf{W}_C\mathbf{W}_C^H + \mathbf{W}_A\mathbf{W}_A^H, \quad (17)$$

which has a full rank of N_t and is now invertible. The CRB of estimating $\mathbf{G}$ is expressed by

$$\begin{aligned}&\mathrm{CRB}\,(\mathbf{G}) = \mathrm{CRB}\,(\mathbf{g}) = \mathrm{CRB}\,(\mathbf{v}) = \mathrm{tr}\left(\mathbf{J}^{-1}\right) \overset{(a)}{=} \frac{\sigma_R^2}{2L}\cdot\\ &\mathrm{tr}\left(\begin{bmatrix}\mathrm{Re}\left(\left(\mathbf{R}_X^{-1}\right)^T \otimes \mathbf{I}_{N_r}\right) & -\mathrm{Im}\left(\left(\mathbf{R}_X^{-1}\right)^T \otimes \mathbf{I}_{N_r}\right)\\ \mathrm{Im}\left(\left(\mathbf{R}_X^{-1}\right)^T \otimes \mathbf{I}_{N_r}\right) & \mathrm{Re}\left(\left(\mathbf{R}_X^{-1}\right)^T \otimes \mathbf{I}_{N_r}\right)\end{bmatrix}\right)\\ &= \frac{\sigma_R^2}{L}\,\mathrm{Re}\left(\mathrm{tr}\left(\left(\mathbf{R}_X^{-1}\right)^T \otimes \mathbf{I}_{N_r}\right)\right) = \frac{\sigma_R^2 N_r}{L}\,\mathrm{Re}\left(\mathrm{tr}\left(\mathbf{R}_X^{-1}\right)\right)\\ &\overset{(b)}{=} \frac{\sigma_R^2 N_r}{L}\,\mathrm{tr}\left(\mathbf{R}_X^{-1}\right),\end{aligned} \quad (18)$$

where (a) is based on the property of the real representation of complex matrices, and (b) is based on the fact that $\mathbf{R}_X$ is a Hermitian matrix, whose diagonal elements are real.

Given the linear Gaussian model in (1), the above CRB is achievable by using maximum likelihood estimation (MLE), i.e., the mean squared error (MSE) of estimating $\mathbf{G}$ is equal to its CRB.

C. SINR for Communication Users

Note that the dedicated probing signals cause interference to the communication users, as $\mathbf{S}_A$ does not contain any useful information. The per-user SINR expression should therefore be expressed as

$$\gamma_k = \frac{\left|\mathbf{h}_k^H\mathbf{w}_k\right|^2}{\sum_{i=1,i\neq k}^K\left|\mathbf{h}_k^H\mathbf{w}_i\right|^2 + \left\|\mathbf{h}_k^H\mathbf{W}_A\right\|^2 + \sigma_C^2}, \quad (19)$$

where the radar interference is imposed in (19) as part of the denominator.

III. Joint Radar-Communication Precoding Design

A. Problem Formulation

Based on the discussion above, the precoding optimization problem can be expressed as

$$\begin{aligned} &\min_{\tilde{\mathbf{W}}_D} \ \mathrm{CRB}\left(\mathbf{G}\right) = \mathrm{tr}\left(\left(\tilde{\mathbf{W}}_D\tilde{\mathbf{W}}_D^H\right)^{-1}\right) \\ &\text{s.t. } \gamma_k \geq \Gamma_k, k=1,\ldots,K, \ \left\|\tilde{\mathbf{W}}_D\right\|_F^2 \leq P_T. \end{aligned} \tag{20}$$

That is, we design a JRC precoder $\tilde{\mathbf{W}}_D$ to minimize the target estimation CRB, while guaranteeing per-user SINR performance. Note that problem (20) depicts a fundamental tradeoff between radar sensing and multi-user communication. Indeed, it can be readily proved that if there are no per-user SINR constraints imposed in (20), the CRB reaches its minimum if and only if $\mathbf{R}_X = \frac{P}{N_t}\mathbf{I}_{N_t}$ [18], in which case $\tilde{\mathbf{W}}_D$ becomes a scaled unitary matrix. By imposing SINR constraints, $\tilde{\mathbf{W}}_D$ might no longer be unitary, resulting in increased CRB. We will further show this tradeoff in our numerical results.

By letting

$$\mathbf{W}_k = \mathbf{w}_k\mathbf{w}_k^H, \forall k \leq K, \quad \mathbf{W}_{K+1} = \mathbf{W}_A\mathbf{W}_A^H, \tag{21}$$

and by dropping the rank-1 constraint on $\mathbf{W}_k, \forall k \leq K$, and rank-$(N_t - K)$ constraint on $\mathbf{W}_{K+1}$, (20) can be relaxed to the following convex form

$$\begin{aligned} &\min_{\{\mathbf{W}_k\}_{k=1}^{K+1}} \ \mathrm{tr}\left(\left(\sum\nolimits_{k=1}^{K+1}\mathbf{W}_k\right)^{-1}\right) \\ &\text{s.t. } \ \mathrm{tr}\left(\mathbf{Q}_k\mathbf{W}_k\right) - \Gamma_k\sum\nolimits_{i=1,i\neq k}^{K+1}\mathrm{tr}\left(\mathbf{Q}_k\mathbf{W}_i\right) \geq \Gamma_k\sigma_C^2, \forall k, \\ &\quad \sum\nolimits_{k=1}^{K+1}\mathrm{tr}\left(\mathbf{W}_k\right) \leq P_T, \mathbf{W}_k \succeq \mathbf{0}, \forall k, \end{aligned} \tag{22}$$

which can be solved by standard numerical tools.

B. SCA Algorithm for Solving Problem (20)

Although the convex relaxation (22) can be optimally solved using numerical tools, solving the SDR formulation could be computationally expensive. Moreover, the rank-1 solution is typically extracted from the SDR solution by Gaussian randomization or eigenvalue decomposition [13], which either requires more computational resources, or may be far from the optimum. To cope with these issues, below we propose an SCA algorithm to directly solve (20).

First of all, note that the SINR constraint (21) can be equivalently rewritten as

$$\begin{aligned} \left(1+\Gamma_k\right)\left|\mathbf{h}_k^H\mathbf{w}_k\right|^2 &\geq \Gamma_k\sum\nolimits_{i=1}^{N_t}\left|\mathbf{h}_k^H\mathbf{w}_i\right|^2 + \Gamma_k\sigma_C^2 \\ &= \Gamma_k\left\|\mathbf{h}_k^H\tilde{\mathbf{W}}_D\right\|^2 + \Gamma_k\sigma_C^2, \end{aligned} \tag{23}$$

which can be formulated into a convex second-order cone (SOC) constraint as follows

$$\sqrt{1+\Gamma_k}\mathbf{h}_k^H\mathbf{w}_k \geq \sqrt{\Gamma_k}\left\|\left[\mathbf{h}_k^H\tilde{\mathbf{W}}_D, \sigma_C\right]\right\|. \tag{24}$$

It is interesting to highlight that the feasibility of (23) indicates that (24) is also feasible, since one can always rotate the phase of $\mathbf{w}_k$ to be aligned with that of the channel $\mathbf{h}_k$ such that $\mathbf{h}_k^H\mathbf{w}_k$ is real and positive. By imposing the SOC formulation (24), one can reformulate (20) as

$$\begin{aligned} &\min_{\tilde{\mathbf{W}}_D} \ f\left(\tilde{\mathbf{W}}_D\right) \triangleq \mathrm{tr}\left(\left(\tilde{\mathbf{W}}_D\tilde{\mathbf{W}}_D^H\right)^{-1}\right) \\ &\text{s.t. } \sqrt{1+\Gamma_k}\mathbf{h}_k^H\mathbf{w}_k \geq \sqrt{\Gamma_k}\left\|\left[\mathbf{h}_k^H\tilde{\mathbf{W}}_D, \sigma_C\right]\right\|, \forall k, \\ &\quad \left\|\tilde{\mathbf{W}}_D\right\|_F^2 \leq P_T. \end{aligned} \tag{25}$$

Denote $\mathcal{Q}$ as the feasible region of problem (25). We observe that the problem is still non-convex despite that $\mathcal{Q}$ is convex, as the objective function $f\left(\tilde{\mathbf{W}}_D\right)$ is non-convex. To proceed with the SCA algorithm, let us approximate the objective function $f\left(\tilde{\mathbf{W}}_D\right)$ by its first-order Taylor expansion near a given point $\tilde{\mathbf{W}}' \in \mathcal{Q}$ as

$$f\left(\tilde{\mathbf{W}}_D\right) \approx f\left(\tilde{\mathbf{W}}'\right) + \mathrm{Re}\left(\mathrm{tr}\left(\nabla f^H\left(\tilde{\mathbf{W}}'\right)\left(\tilde{\mathbf{W}}_D - \tilde{\mathbf{W}}'\right)\right)\right), \tag{26}$$

where $\nabla f\left(\cdot\right)$ represents the gradient of $f\left(\cdot\right)$, and can be calculated as

$$\nabla f\left(\tilde{\mathbf{W}}_D\right) = -2\left(\tilde{\mathbf{W}}_D\tilde{\mathbf{W}}_D^H\right)^{-1}\left(\tilde{\mathbf{W}}_D\tilde{\mathbf{W}}_D^H\right)^{-1}\tilde{\mathbf{W}}_D. \tag{27}$$

At the i-th iteration of the SCA algorithm, we solve the following convex optimization problem

$$\begin{aligned} &\min_{\tilde{\mathbf{W}}_D} \ g\left(\tilde{\mathbf{W}}_D\right) \triangleq \mathrm{Re}\left(\mathrm{tr}\left(\nabla f^H\left(\tilde{\mathbf{W}}_D^{i-1}\right)\left(\tilde{\mathbf{W}}_D - \tilde{\mathbf{W}}_D^{i-1}\right)\right)\right) \\ &\text{s.t. } \sqrt{1+\Gamma_k}\mathbf{h}_k^H\mathbf{w}_k \geq \sqrt{\Gamma_k}\left\|\left[\mathbf{h}_k^H\tilde{\mathbf{W}}_D, \sigma_C\right]\right\|, \forall k, \\ &\quad \left\|\tilde{\mathbf{W}}_D\right\|_F^2 \leq P_T, \end{aligned} \tag{28}$$

where $\tilde{\mathbf{W}}_D^{i-1} \in \mathcal{Q}$ is the obtained point at the $(i-1)$-th iteration. By solving problem (28) we reach to an optimal solution $\tilde{\mathbf{W}}_D^* \in \mathcal{Q}$. It is obvious that $g\left(\tilde{\mathbf{W}}_D^*\right) \leq 0$, since $g\left(\tilde{\mathbf{W}}_D^{i-1}\right) = 0$. Therefore, $\tilde{\mathbf{W}}_D^* - \tilde{\mathbf{W}}_D^{i-1}$ yields a descent direction for the i-th iteration. Next, we move along the descent direction with a stepsize t to get the updated point $\tilde{\mathbf{W}}_D^i$. This is expressed as

$$\tilde{\mathbf{W}}_D^i = \tilde{\mathbf{W}}_D^{i-1} + t\left(\tilde{\mathbf{W}}_D^* - \tilde{\mathbf{W}}_D^{i-1}\right), \quad t \in [0,1]. \tag{29}$$

It is straightforward to see that $\tilde{\mathbf{W}}_D^i \in \mathcal{Q}$, since both $\tilde{\mathbf{W}}_D^{i-1}$ and $\tilde{\mathbf{W}}_D^*$ are drawn from the convex set $\mathcal{Q}$.

The performance of Algorithm 1 critically hinges on the choice of $\mathbf{W}_D^0$. To find a good initial point, one may solve the following convex problem

$$\begin{aligned} &\max_{\tilde{\mathbf{W}}_D} \ \mathrm{Re}\left(\mathrm{tr}\left(\tilde{\mathbf{W}}_D\right)\right) \\ &\text{s.t. } \sqrt{1+\Gamma_k}\mathbf{h}_k^H\mathbf{w}_k \geq \sqrt{\Gamma_k}\left\|\left[\mathbf{h}_k^H\tilde{\mathbf{W}}_D, \sigma_C\right]\right\|, \forall k, \\ &\quad \left\|\tilde{\mathbf{W}}_D\right\|_F^2 \leq P_T. \end{aligned} \tag{30}$$

Note that the objective in (30) is to maximize the trace of $\tilde{\mathbf{W}}_D$. In general, this could result in an initial point that is close to the minimizer of $f\left(\tilde{\mathbf{W}}_D\right)$ in (25).

We are now ready to present our SCA approach for solving (25), which is summarized in Algorithm 1.

Algorithm 1 SCA Algorithm for Solving (25)

Input: $\mathbf{H}$, P_T, $\Gamma_k, \forall k$, $\varepsilon > 0$, and the maximum iteration number $i_{\max}$

Output: $\tilde{\mathbf{W}}_D$

1. Solve the convex problem (30) to obtain $\tilde{\mathbf{W}}_D^0 \in \mathcal{Q}$, $i = 1$.

while $i \leq i_{\max}$ and $g\left(\tilde{\mathbf{W}}_D^i\right) \leq -\varepsilon$ **do**

2. Solve problem (28) to obtain $\mathbf{W}_D^*$, with the gradient being set as $\nabla f\left(\tilde{\mathbf{W}}_D^{i-1}\right)$.

3. Update the solution by

$$\tilde{\mathbf{W}}_D^i = \tilde{\mathbf{W}}_D^{i-1} + t\left(\tilde{\mathbf{W}}_D^* - \tilde{\mathbf{W}}_D^{i-1}\right),$$

where t can be found by using the Armijo or the exact line search.

4. $i = i + 1$.

end while

C. Convergence Property and Complexity Analysis

We note here that Algorithm 1 is a type of the Frank-Wolfe algorithm [19], which lies in the framework of feasible descent algorithms. Together with a careful line search, Algorithm 1 is guaranteed to converge to a stationary point of the optimization problem [19]. Our simulations show that Algorithm 1 converges to a near-optimal point with less than 10 iterations at a modest accuracy.

A simple analysis shows that, to achieve the same accuracy, solving the SOCP (28) and the SDP formulation of (22) has worst-case arithmetic complexities of $\mathcal{O}\left(K^{0.5}N_t^6\right)$ and $\mathcal{O}\left(K^{3.5}N_t^{6.5}\right)$, respectively [20]. This suggests that the SCA algorithm performs considerably more efficient than the SDR solver, despite that it requires a number of SOCP iterations.

IV. Numerical Results

In this section, we provide numerical results to verify the superiority of the proposed joint precoding approaches. Without loss of generality, we consider a JRC BS that is equipped with $N_t = 16$ and $N_r = 20$ antennas for its transmitter and receiver. The power budget is $P_T = 30$dBm, the noise variances are set as $\sigma_C^2 = \sigma_R^2 = 0$dBm, and the JRC frames length is set as $L = 30$. Without loss of generality, we have $\Gamma_k = \Gamma, \forall k$, i.e., all the communication users are imposed with the same worst-case QoS. Moreover, we assume that the entries of the target response matrix $\mathbf{G}$ are i.i.d. Gaussian distributed with zero mean and unit variance, which corresponds to a Swerling 1 or Swerling 2 extended target with Gaussian distributed complex amplitude for each of the scatterers, or to a large number of Swerling 1-2 type point targets [21]. This represents the case that there are a large number of reflecting paths from the target(s) to the BS, whose overall summation leads to the Gaussian distributed complex path gain thanks to the Central-Limit Theorem.

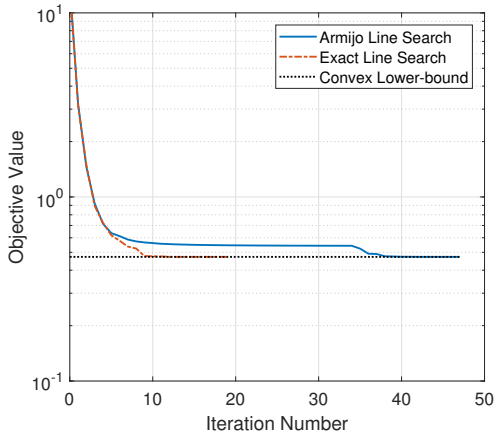

Fig. 2. Convergence performance of the proposed SCA algorithm, $K = 10$ and $\Gamma_k = 20$dB, $\forall k$.

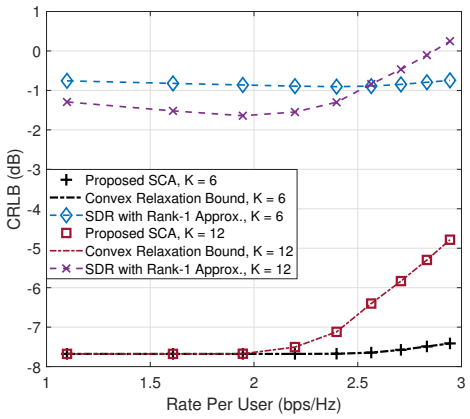

Fig. 3. Tradeoff between target estimation CRB and communication rate per user, in the cases of $K = 12$ and $K = 6$. The rank-1 approximation for the SDR (22) is serving as the benchmark.

Let us first look at the convergence performance of the proposed SCA algorithm in Fig. 2, where the tolerance threshold of the algorithm is set as $\varepsilon = 10^{-6}$, with $K = 10$ users, whose SINR threshold is $\Gamma_k = 20$dB, $\forall k$. It is surprising to see that the SCA algorithm is able to approach the convex relaxation lower bound, i.e., the solution attained from solving the SDR problem (22). Without loss of generality, we test both the Armijo and exact line search methods, both of which are able to converge to the optimum within tens of iterations. While it is well-known that the Armijo line search is able to find a feasible stepsize more efficiently, it generally needs more iterations to reach the optimum compared to that of the exact line search [22]. Given the fact that the solution is updated by solving (28) for each iteration, whose complexity is much higher than that of the 1-dimensional line search, the exact line search method is more efficient in terms of the overall computational complexity.

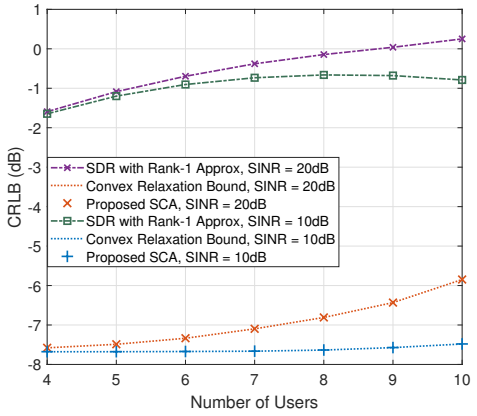

Fig. 4. Target estimation CRB versus user number, with the SINR being set as 20dB and 10dB. The rank-1 approximation for the SDR (22) is serving as the benchmark.

In Fig. 3, we plot the performance tradeoff between the target estimation CRB and the communication rate per user with $K = 12$ and 6, respectively. In particular, the per user rate is translated from the SINR constraint as $\log(1+\Gamma)$ bps/Hz. The rank-1 approximation of the SDR problem (22) is employed as a benchmark, which is obtained by applying the eigenvalue decomposition on the solution of (22). We see that the proposed SCA technique is superior to the SDR with rank-1 approximation method by achieving the optimal performance bound. On the other hand, the rank-1 approximation fails to generate a favorable performance tradeoff between MSE and SINR, as the trends of the corresponding tradeoff curves are not monotonically increasing. More interestingly, the CRB for the proposed SCA remains at a small level despite that the SINR requirement is increasing, given a moderate number of users, e.g., $K = 6$.

Finally in Fig. 4, we show the impact of the communication user number imposed on the radar estimation performance, with the SINR being set as $\Gamma = 20$dB and $\Gamma = 10$dB, respectively. It is observed that when the user number is on the rise, the estimation performance becomes worse. Fortunately, the variation of the CRB can be kept within 1dB when the required SINR is 10dB. Again, the results prove the superiority of the proposed SCA algorithm over that of the SDR with rank-1 approximation.

V. Conclusion

In this paper, we proposed a novel precoding design for joint radar sensing and multi-user communications. In particular, we formulated optimization problems to minimize the CRB of target estimation by imposing SINR constraints for multiple communication users. While the multi-user JRC precoding problem is non-convex, we solve it by using a specifically tailored SCA algorithm. Numerical results demonstrated that the proposed approach yields near-optimal solution by approaching the convex relaxation bound, while significantly outperforming the benchmark techniques in terms of the target estimation performance and the complexity.

References

[1] F. Liu, Y. Cui, C. Masouros, J. Xu, T. X. Han, Y. C. Eldar, and S. Buzzi. (2021) Integrated sensing and communications: Towards dual-functional wireless networks for 6G and beyond. Submitted to *IEEE J. Sel. Areas. Commun.* [Online]. Available: https://arxiv.org/abs/2108.07165

[2] F. Liu, C. Masouros, A. Petropulu, H. Griffiths, and L. Hanzo, "Joint radar and communication design: Applications, state-of-the-art, and the road ahead," *IEEE Trans. Commun.*, vol. 66, no. 6, pp. 3834–3862, Jun. 2020.

[3] A. Hassanien, M. G. Amin, Y. D. Zhang, and F. Ahmad, "Dual-function radar-communications: Information embedding using sidelobe control and waveform diversity," *IEEE Trans. Signal Process.*, vol. 64, no. 8, pp. 2168–2181, Apr. 2016.

[4] T. Huang, N. Shlezinger, X. Xu, D. Ma, Y. Liu, and Y. C. Eldar, "Multi-carrier agile phased array radar," *IEEE Trans. Signal Process.*, vol. 68, pp. 5706–5721, 2020.

[5] T. Huang, N. Shlezinger, X. Xu, Y. Liu, and Y. C. Eldar, "MAJoRCom: A dual-function radar communication system using index modulation," *IEEE Trans. Signal Process.*, vol. 68, pp. 3423–3438, 2020.

[6] D. Ma, N. Shlezinger, T. Huang, Y. Liu, and Y. C. Eldar. (2021) "FRaC: FMCW-based joint radar-communications system via index modulation". Submitted to *IEEE Trans. Signa Process.* [Online]. Available: https://arxiv.org/abs/2106.14671

[7] C. Sturm and W. Wiesbeck, "Waveform design and signal processing aspects for fusion of wireless communications and radar sensing," *Proc. IEEE*, vol. 99, no. 7, pp. 1236–1259, Jul. 2011.

[8] P. Kumari, J. Choi, N. González-Prelcic, and R. W. Heath, "IEEE 802.11ad-based radar: An approach to joint vehicular communication-radar system," *IEEE Trans. Veh. Technol.*, vol. 67, no. 4, pp. 3012–3027, Apr. 2018.

[9] E. Grossi, M. Lops, L. Venturino, and A. Zappone, "Opportunistic radar in IEEE 802.11ad networks," *IEEE Trans. Signal Process.*, vol. 66, no. 9, pp. 2441–2454, May 2018.

[10] F. Liu, L. Zhou, C. Masouros, A. Li, W. Luo, and A. Petropulu, "Toward dual-functional radar-communication systems: Optimal waveform design," *IEEE Trans. Signal Process.*, vol. 66, no. 16, pp. 4264–4279, Aug. 2018.

[11] X. Liu, T. Huang, N. Shlezinger, Y. Liu, J. Zhou, and Y. C. Eldar, "Joint transmit beamforming for multiuser MIMO communications and MIMO radar," *IEEE Trans. Signal Process.*, vol. 68, pp. 3929–3944, 2020.

[12] F. Liu, Y.-F. Liu, A. Li, C. Masouros, and Y. C. Eldar. (2021) "Cramér-Rao bound optimization for joint radar-communication design". Submitted to *IEEE Trans. Signa Process.* [Online]. Available: https://arxiv.org/abs/2101.12530

[13] Z. -Q. Luo, W. -K. Ma, A. M. -C. So, Y. Ye, and S. Zhang, "Semidefinite relaxation of quadratic optimization problems," *IEEE Signal Process. Mag.*, vol. 27, no. 3, pp. 20–34, May 2010.

[14] B. Tang and J. Li, "Spectrally constrained MIMO radar waveform design based on mutual information," *IEEE Trans. Signal Process.*, vol. 67, no. 3, pp. 821–834, Feb. 2019.

[15] S. M. Kay, *Fundamentals of Statistical Signal Processing, Vol. I: Estimation Theory*. Englewood Cliffs, NJ, USA: Prentice Hall, 1998.

[16] P. Stoica and T. L. Marzetta, "Parameter estimation problems with singular information matrices," *IEEE Trans. Signal Process.*, Jan. 2001.

[17] Z. Ben-Haim and Y. C. Eldar, "On the constrained Cramér–Rao bound with a singular Fisher information matrix," *IEEE Signal Process. Lett.*, vol. 16, no. 6, pp. 453–456, Jun. 2009.

[18] F. Liu and C. Masouros, "Joint beamforming design for extended target estimation and multiuser communication," in *2020 IEEE Radar Conference (RadarConf20)*, 2020, pp. 1–6.

[19] S. Lacoste-Julien and M. Jaggi, "On the global linear convergence of Frank-Wolfe optimization variants," in *Advances in neural information processing systems*, 2015, pp. 496–504.

[20] A. Ben-Tal and A. S. Nemirovskiaei, *Lectures on Modern Convex Optimization: Analysis, Algorithms, and Engineering Applications*. USA: Society for Industrial and Applied Mathematics, 2001.

[21] M. A. Richards, *Fundamentals of radar signal processing*. McGraw-Hill Education, 2014.

[22] S. Boyd and L. Vandenberghe, *Convex Optimization*. Cambridge University Press, 2004.